A VO2 based hybrid super-capacitor utilizing a highly concentrated aqueous electrolyte for increased potential window and capacity

Electrochimica Acta 345 (2020) 136225

Contents lists available at ScienceDirect

Electrochimica Acta

journal homepage: www.elsevier.com/locate/electacta

A VO_2 based hybrid super-capacitor utilizing a highly concentrated aqueous electrolyte for increased potential window and capacity

Simon Lindberg [a], Ndeye Maty Ndiaye [b], Ncholu Manyala [b], Patrik Johansson [a], Aleksandar Matic [a, *]

[a] Department of Physics, Chalmers University of Technology, 41296, Göteborg, Sweden
[b] Department of Physics, Institute of Applied Materials, University of Pretoria, Pretoria, 0028, South Africa

ARTICLE INFO

Article history:
Received 27 January 2020
Received in revised form
23 March 2020
Accepted 8 April 2020
Available online 12 April 2020

Keywords:
Highly concentrated electrolyte
NaTFSI
VO2
Supercapacitor
Stability

ABSTRACT

In this work we demonstrate the application of a highly concentrated aqueous electrolyte to a hybrid supercapacitor cell. We combine an 8 m Sodium bis(trifluoromethanesulfonyl)imide (NaTFSI) aqueous electrolyte with a nanostructured VO_2-cathode to enhance the voltage widow up to 2.4 V in a full cell. With the enhanced potential window, we are able to exploit the full contribution of the VO_2 material, where a part is outside the stability window of standard alkaline aqueous electrolytes. We show that the VO_2 material in the highly concentrated electrolyte provides a faradaic contribution even at the highest current density (25 A/g) and in this way increases the energy content also in high power conditions. The full cell shows a good efficiency but also a capacity fade over 500 cycles (39%) which is most likely related to dissolution of VO_2.

1. Introduction

There has in recent years been considerable efforts devoted to increase the energy content of supercapacitors to meet the demand by applications where both power and energy are needed. One route to achieve this is adding electrochemically active materials, such as MnO_2 or RuO_2, to the electrodes, to also exploit faradaic contributions to the capacity, in addition to the electric double layer, in a hybrid device [1,2]. Typically, a standard electrode with activated carbon (AC) has a specific capacity in the range of 33 mAh/g [3,4] while a MnO_2 electrode has a specific capacity up to 308 mAh/g [5], both in neutral aqueous electrolytes. A second route explored is to increase the voltage widow since the energy content of a supercapacitor is proportional to the potential window squared [6]. This is illustrated by comparing the performance of an electric double layer capacitor (EDLC) using a high voltage electrolyte, up to more than 30 Wh/kg with a cell voltage up to 3.5 V [7], compared to cells with aqueous based electrolytes with cell voltage up to 1.6 V and energy content around 10 Wh/kg [8]. One way to achieve even higher energy content is to combine electrolytes with larger electrochemical stability with electrochemically active electrodes. This concept has for instance been demonstrated by Zhang et al. using a Fe_3O_4-graphene nanocomposite electrode and an organic solvent based electrolyte (ethylene carbonate, diethyl carbonate and dimethyl carbonate) with a cell voltage around 3 V [9]. However, organic solvent electrolytes are flammable which introduces safety concerns and increases the electrolyte cost compared to water-based electrolytes. Thus, there is an interest to investigate new electrolyte systems with the possibility to combine a larger voltage window with the safety and environmental friendliness of aqueous electrolytes.

Highly concentrated aqueous electrolytes [6,10,11], with salt concentrations considerably above the standard concentration of about 1 M, have gained considerable interest, due to the increased electrochemical stability window compared to traditional aqueous electrolytes and improved safety and less toxicity compared to organic solvent electrolytes [12]. The increased electrochemical stability originates from the fact that all solvent molecules (water) will be engaged in coordinating the ions and thereby leading to a suppression of water splitting at higher potential [13]. A standard aqueous electrolyte would start to decompose around 1.3–1.5 V, whereas highly concentrated electrolytes have been shown to be stable up to 3 V [14], depending on type of salt and salt concentration. Thus, a supercapacitor utilizing a highly concentrated

* Corresponding author.
E-mail address: matic@chalmers.se (A. Matic).

https://doi.org/10.1016/j.electacta.2020.136225

electrolyte can be cycled in a wider potential window, resulting in an increase in the energy density of the cell.

Increasing the salt concentration, however, also lowers the conductivity of the electrolyte and for supercapacitors this is detrimental for the power density. For optimal power performance both the potential window and conductivity need to be optimized by tuning the salt concentration. Battaglia et al. investigated the performance as a function of salt concentration of symmetric carbon/carbon cells using an aqueous NaTFSI electrolyte and found 8 m NaTFSI (corresponding to 3.75 M) to be an optimal concentration, balancing electrochemical stability and conductivity to optimize the power performance [11]. This can be compared with the concentrations reported for highly concentrated electrolytes in battery applications around 21 m [12,14]. For higher concentrations the power performance is limited by the conductivity whereas at lower concentrations the voltage window was not significantly enhanced.

To develop this approach further we have in this work investigated the interaction between the 8 m NaTFSI aqueous electrolyte and a faradaic cathode, based on nanostructured VO_2, in a hybrid supercapacitor cell. VO_2 materials in general show good specific capacity using aqueous electrolytes [15–17], however, in some studies with a limited cycle performance [15]. The capacity fade has been attributed to chemical dissolution [18] as well as other mechanisms induced by the intercalation/extraction of ions, such as destroyed particle morphologies during cycling [19]. Here we investigate the useful potential window, capacity retention and efficiency of a VO_2 cathode material when combined with the highly concentrated electrolyte as well as demonstrating its application in a full hybrid cell with an activated carbon anode.

2. Experimental

NaTFSI (99.5%, Solvionic), Activated carbon (AC) (Darco G-60, 600 m^2/g, 0.95 ml/g), polyvinylidene fluoride (PVdF), carbon black (both from Sigma-Aldrich) were all used as received. To prepare the electrolyte NaTFSI was mixed with milliQ water.

The VO_2 active material was synthesized according to the previously published procedure using a solvothermal method for either 2.5 or 4 h [17]. SEM images of the as prepared VO_2 material were acquired on a high-resolution Zeiss Ultra Plus 55 scanning electron microscope (SEM) operated at a voltage of 2.0 kV. Electrodes were prepared by grinding-mixing the active material (80%), carbon black (10%) and PVdF (10%) with NMP in a mortar for 10 min. The slurry was then applied to the stainless steel current collector and dried at 60 °C overnight.

T-shaped Teflon cells, with stainless steel rods as current collectors were used for all electrochemical measurements. The electrode projected area was 0.785 cm^2 and the mass loading varied between 1.1 and 1.8 mg/cm^2, which could be considered quite low compared to the mass loading of AC in state-of-the-art supercapacitors which is around 10 mg/cm^2 [20]. The activated carbon electrodes had similar mass loading as the VO_2 electrodes in the 3-electrode measurements and approximately the double in the full cell measurements. Filter paper was used as separator. Ag/AgCl was used as reference in a saturated KCl-solution with a fresh Vycor-tip attached at the end of the reference container. The counter electrode was prepared by oversizing an AC-electrode.

The electrochemical measurements were performed on a Bio-Logic VMP3 electrochemical workstation. Scan speeds between 10 and 200 mV/s were used for cyclic voltammetry (CV) and in constant current (CC) cycling current densities between 2 and 25 A/g, with respect to total electrode weight, were used to ensure that both the high energy and high-power performances were evaluated. Rate tests were performed in the potential windows of 0 to −1.2 V and 0–1.2 V for the AC and the VO_2 electrodes, respectively, in the 8 m NaTFSI aqueous electrolyte and between 0 and 0.5 V in the 6 M KOH electrolyte for the VO_2 electrode. The

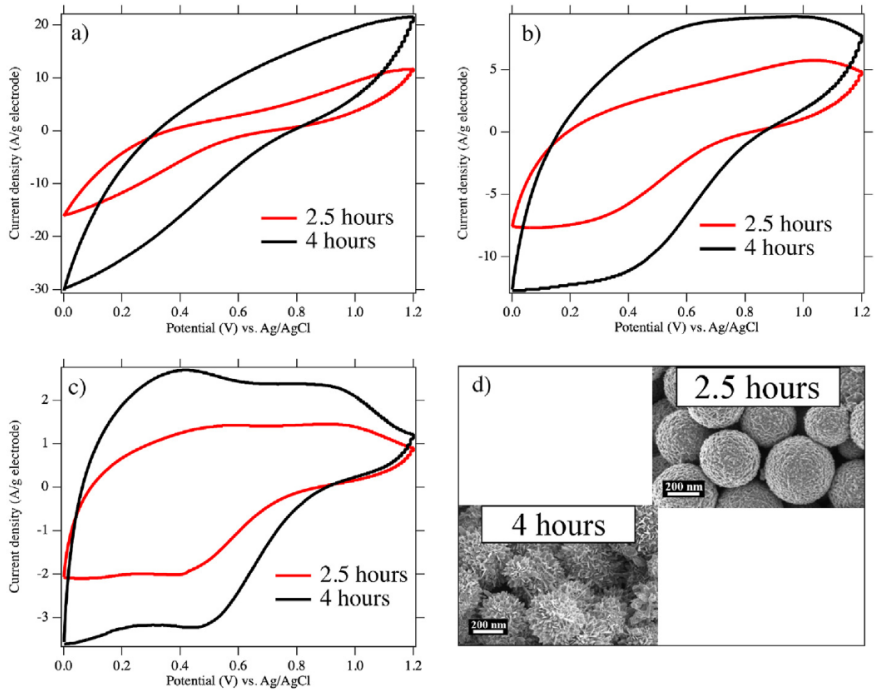

Fig. 1. CV response of VO_2 electrodes with materials synthesized for 2.5 and 4 h, respectively, with the highly concentrated electrolyte a) 200 mV/s, b) 50 mV/s and c) 10 mV/s d) SEM images of the as prepared materials.

cut-off voltage for the highly concentrated electrolyte was set to 1.2 V since no additional peaks appeared at higher potentials and expanding the voltage window further did not improve the capacity. The upper potential of the alkaline electrolyte was set to 0.5 V to avoid hydrogen or oxygen evolution at higher voltage promoted by pH-changes at the surface of the electrodes [21]. Balanced electrodes were prepared for the full cell with respect to their specific capacity determined at a current density of 25 A/g.

3. Results and discussion

The morphology of the VO_2 materials depends heavily on the reaction time during solvothermal synthesis [17]. Thus, initially the morphology of the two VO_2 materials, processed for 2.5 and 4 h respectively, and the electrochemical properties, when used with the highly concentrated electrolyte, were characterized. Subsequently the best performing material was evaluated in a half-cell with the highly-concentrated electrolyte and its applicability demonstrated in a full, asymmetric cell.

In Fig. 1 SEM images of the two materials show that both are built up of 200 nm diameter spheres, but with different surface morphology. The material processed for 2.5 h has nanorods on the surface and a specific surface area of 16 m^2/g, while the material processed for 4 h has a rougher surface with nanoflakes and a larger surface area, 24 m^2/g. It has previously been reported that the difference in processing time also can result in a slight difference in crystal structure [9,10]. Both materials are expected to be monoclinic, but with a slight increase in lattice parameters with processing time. Both the morphology and the crystal structure are expected to influence the electrochemical response of the material.

Fig. 1 shows the CV response for the two VO_2-materials with the highly concentrated electrolyte at different scan rates (10–200 mV/s). The response for both materials deviates substantially from the typical square shape related to a double layer capacitance contribution. The broad peaks around 0.4 and 1 V at low scan rate, Fig. 1c, show that VO_2 adds a faradaic contribution to the capacity. With increasing scan rate, the peaks become less pronounced but can still be discerned at 200 mV/s, Fig. 1a.

Even though both materials have similar CV characteristics the current response is consistently higher for the material processed for 4 h. This difference in performance can be attributed to the difference in surface area and is in agreement with previously reported results using a 6 M KOH aqueous electrolyte [17]. The difference in surface area is especially important at faster scan rates, when the reactions are limited to the surface, and explains the larger difference in current response at the highest scan speed, 200 mV/s. At slower scan rates the contribution from the faradaic reactions becomes more important. The increased current for the 4 h material can also in this case be partly related to the larger surface area since more VO_2-units are available for electrochemical reactions. However, there could also be a contribution related to the increase in lattice parameters allowing easier insertion/extraction of Na-ions. One can note that the shape of the CV for the VO_2 electrode in the 8 m NaTFSI electrolyte is very similar to the CV when using a 1 M $LiClO_4$ propylene carbonate electrolyte with VO_2 [22], which could indicate that the insertion/extraction processes for Na^+ and Li^+ are similar and with slower kinetics of both electrolytes compared to standard aqueous electrolytes.

Based on the increased current response the VO_2 material processes for 4 h was chosen to further investigate the functionality of the highly concentrated electrolyte. In Fig. 2 the CV response of the VO_2-electrode using the highly concentrated 8 m NaTFSI electrolyte and a standard 6 M KOH electrolyte are compared at two different scan speeds. The current responses for the two electrolytes have very different characteristics. The 6 M KOH electrolyte displays clear peaks in the CV, at 0.25 and 0.15 V for oxidation and reduction, respectively, indicating fast kinetics, further underlined by the relatively small shifts and broadenings as the scan speed is increased. The rapid current increase at 0.5 V indicates electrolyte decomposition and that the end of the stable potential window has been reached.

In contrast, the current response when using the 8 m NaTFSI

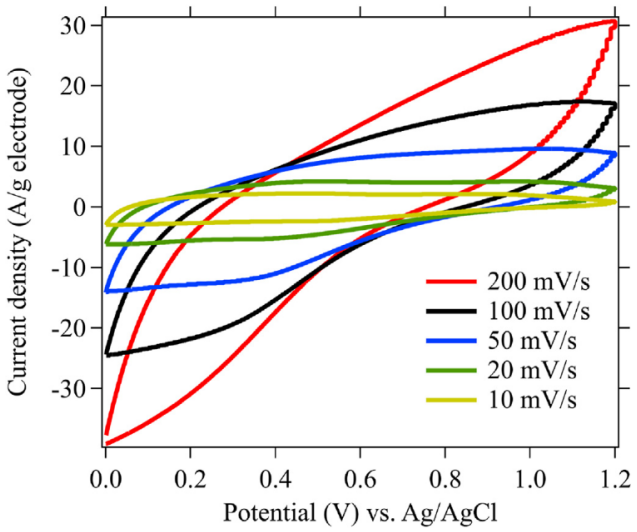

Fig. 3. CV response at different scan rates of the VO_2-electrode in cells with the highly concentrated electrolyte.

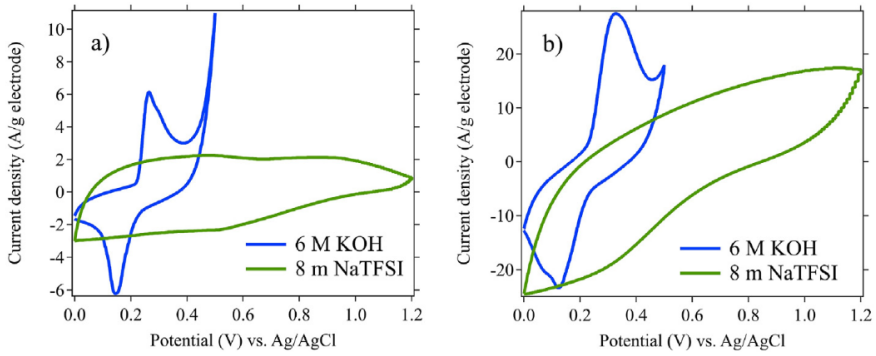

Fig. 2. Comparison of CV response of VO_2 electrodes in 6 M KOH and 8 m NaTFSI electrolytes at scan rates a) 10 mV/s and b) 100 mV/s.

electrolyte displays much broader peaks, at 0.4 and 0.9 V for oxidation and reduction, respectively, which are barely visible at higher scan rates. The peak at 0.9 V (10 mV/s) during oxidation and the shoulder at 0.6 V during reduction can only be seen with the highly concentrated electrolyte since it is outside the stability window for the KOH-based electrolyte. This demonstrates that the highly concentrated electrolyte has an increased potential window compared to the alkaline electrolyte resulting in both an increased energy contribution from the non-faradic double layer capacity as well as enabling the exploitation of the full faradaic contribution of the VO_2 material.

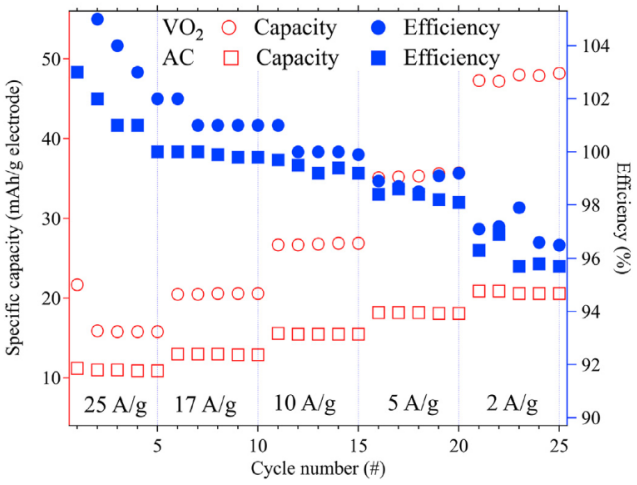

Fig. 4. Specific capacity and efficiency of VO_2- and AC-electrodes with the highly concentrated electrolyte.

The broadening of the peaks in the CV when using the highly concentrated electrolyte indicate slower kinetics of the faradaic process. The slower kinetics can be an effect of the lower conductivity of the 8 m NaTFSI electrolyte (σ = 48 mS/cm [11]) compared to the 6 M KOH electrolyte (σ = 600 mS/cm [23]). An additional factor that can influence the CV is the characteristics of the ions in the electrolyte. Na^+ is smaller than K^+, even in its hydrated form, 1.02–1.07 Å and 1.38–1.46 Å respectively [24] and the smaller size of Na^+ could favor efficient insertion into VO_2. However, the anions are also very different. The OH^- will increase the pH of the electrolyte and is also very mobile [23] whereas the TFSI anion will coordinate strongly with the Na-ions [12], which slows down the insertion process. These factors are most likely also part of the explanation of the smeared out peaks in the CV at higher scan speed for the cell with the highly concentrated electrolyte.

The effect of scan rate on the CV response for cells with the highly concentrated electrolyte is reported in Fig. 3. Increasing the scan rate gradually tilts the curves, which is related to an increased the resistivity of the system. This is further underlined by an increase in the internal resistance (IR) drop at faster scan rate, which discussed in detail below, Fig. 5. However, even at the highest scan rate, 200 mV/s, a small faradaic contribution to the total capacity can be observed since the CV response is not completely linear, as seen in Fig. 3.

To assess the capacity of the VO_2-material in the highly concentrated electrolyte, the 3-electrode setup was cycled at constant current densities of 25, 17 and 2 A/g, and compared to the performance of commercial activated carbon in the same electrolyte, Fig. 4. The capacity of the VO_2 electrode is considerably higher than that of the AC-electrode at low scan rates but the capacity retention is worse, loosing 79% of the specific capacity when going from 2 to 25 A/g, compared to 50% for AC-electrode. This difference can be attributed to the higher surface area and the higher

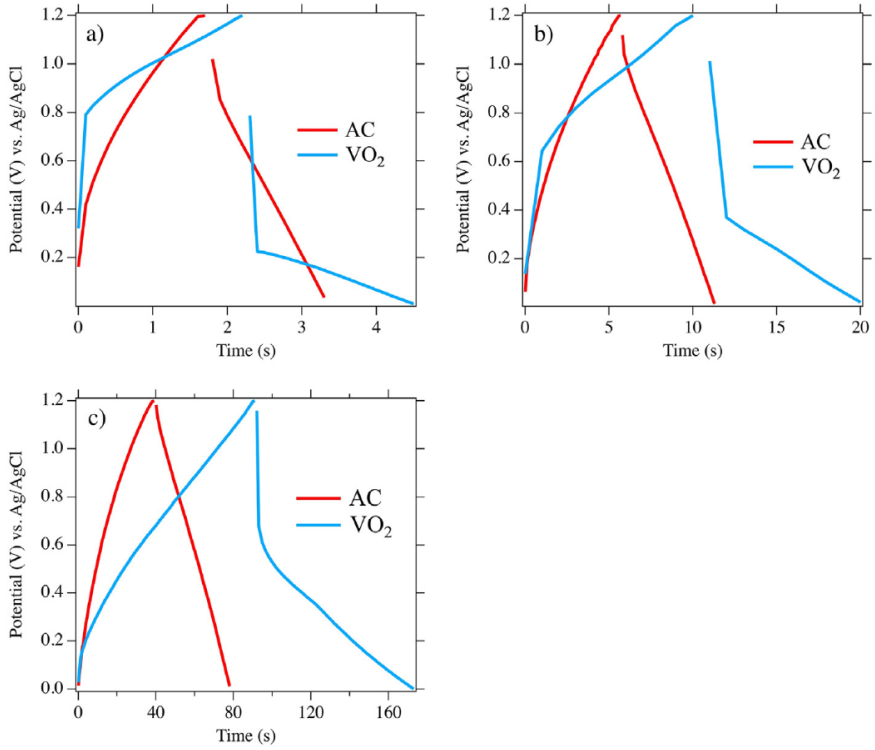

Fig. 5. Potential profiles during constant current charge/discharge at a) 25 A/g, b) 10 A/g and c) 2 A/g of the VO_2- and AC electrodes with the highly concentrated electrolyte.

conductivity of activated carbon and that a large part of the capacity at low current densities comes from slower faradaic insertion processes. One can note that the specific capacity is still higher for the VO_2 electrode at the highest current density (25 A/g) showing that also at this very high current density there is a small faradaic contribution. The coulombic efficiency is high and comparable for both electrodes. Initially it is above 100% which could be explained by irreversible changes on the surfaces of the electrodes or interaction with oxides on the current collectors.

To further investigate the response of the VO_2- and AC-electrodes with the highly concentrated electrolyte, the voltage profiles in constant current experiments are compared in Fig. 5. The voltage profiles from the experiments using the VO_2-electrodes show a clear non-linearity connected to the faradaic processes in the charge storage mechanism compared to the linear profile of the response from the activated carbon electrode which has only a double layer contribution. There is also a difference in the CC-response concerning the IR-drop. At 25 A/g an IR-drop of about 0.32 V is found for the VO_2-electrode, while the AC-electrode shows a smaller drop, 0.18 V. At 2 A/g this difference has almost disappeared underlining the importance of the conductivity of the electrode material at high current densities.

To assess the cycle lifetime of the VO_2-electrode with the highly concentrated electrolyte, it was cycled in a 3-electrode setup 500 times at 25 A/g. The results are shown in Fig. 6 with the specific capacity and the efficiency of the electrode calculated every 25th cycle. There is a clear capacity fade and over the first 400 cycles the capacity is reduced by 39%, but then stabilizes. The capacity fade can be related to slow dissolution of VO_2 into the electrolyte as a result of slightly acidic conditions [18] and is in line with literature results on comparableVO_2-electrodes [15]. The coulombic efficiency of the cell only decreases 4% during 500 cycles.

To demonstrate the applicability of VO_2 material in combination with the highly concentrated electrolyte in a hybrid supercapacitor device it was investigated in a full cell configuration with activated carbon as anode material. By combining the VO_2-cathode with the AC-anode and using the highly concentrated electrolyte it is possible to obtain a full cell potential of 2.4 V. To assemble a full cell the capacities of the VO_2-cathode and the AC-anode need to be determined in order to balance the cell, thus the two electrodes were characterized separately in their corresponding potential windows, Fig. 7. At 25 A/g the VO_2 electrode has a specific capacity 1.4 times higher than the AC-anode, hence in the full cell the weight of the AC-electrode was 1.4 times higher. Fig. 8 shows the capacity retention and the efficiency of the VO_2/8 m NaTFSI/AC full cell over 500 cycles. The retention for the full cell is slightly better than for the individual VO_2-electrode. The full cell loses around 35% of the initial capacity over 500 cycles. However, the efficiency is still quite good and is approaching 99% during cycling.

4. Conclusions

We show that by using a neutral highly concentrated aqueous electrolyte it is possible to expand the upper potential limit

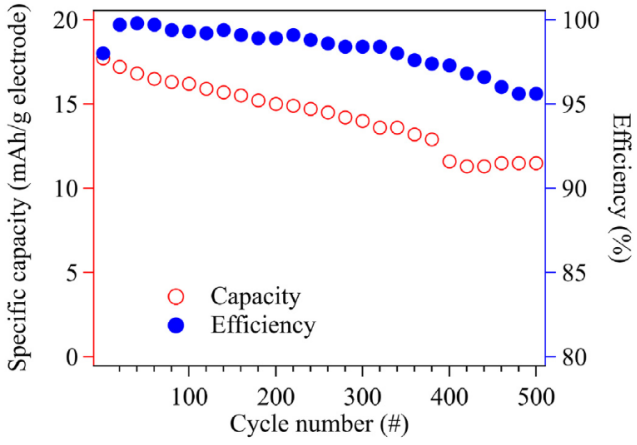

Fig. 6. Cycle lifetime and efficiency of VO_2 during 500 cycles at 25 A/g.

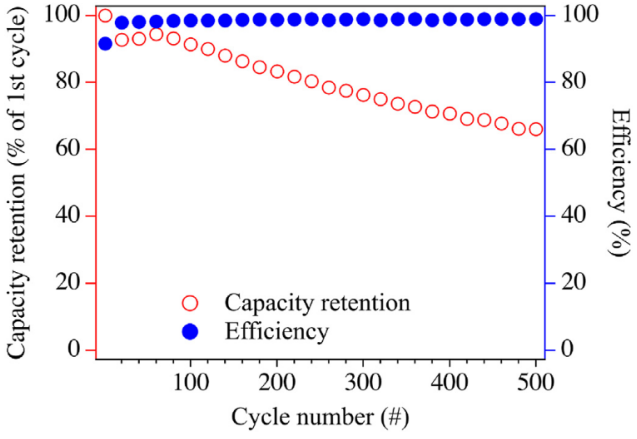

Fig. 8. Capacity retention and efficiency of the VO_2/AC full cell with the highly concentrated electrolyte at current density of 25 A/g.

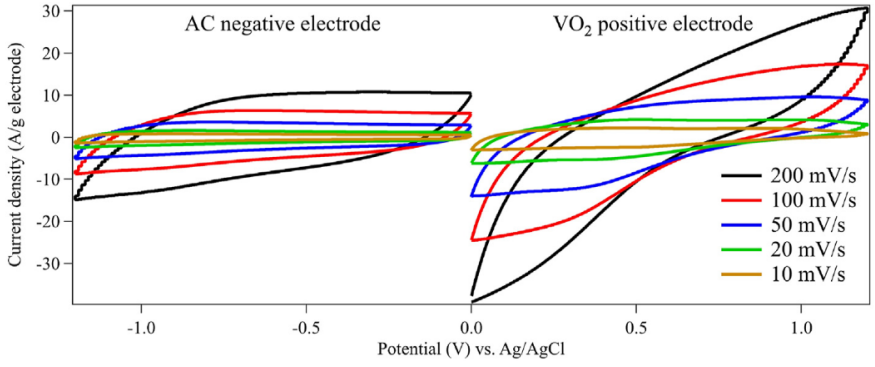

Fig. 7. CVs of carbon anode and VO_2 cathode making up a 2.4 V full cell.

compared to aqueous alkaline electrolytes, from 0.5 to 1.2 V, in a hybrid supercapacitor application resulting in a full cell voltage of 2.4 V. An 8 m NaTFSI highly concentrated electrolyte is combined with a faradaic VO_2 material which results in a higher capacity compared to a standard KOH electrolyte, even though the conductivity of the 8 m NaTFSI electrolyte is lower. The mechanism behind the increased capacity is related to the faradaic process with insertion of Na^+ in the VO_2 structure. The CC-potential profiles clearly show, non-linear, behavior typical of battery-type, or faradaic materials, compared to the linear profiles typically observed for non-faradic materials, such as activated carbons. At high rates the difference decreases as the faradaic process is limited by kinetics.

The cycle lifetime of the VO_2 material in the highly concentrated electrolyte is lower compared to KOH or other neutral electrolytes. Previous studies have shown a dependence on the pH of the dissolution of VO_2 [18]. Since the highly concentrated electrolyte could be slightly acidic, one can connect the lower capacity retention to VO_2 dissolution in the electrolyte. Thus, the use of a highly concentrated NaTFSI-based electrolyte will require the addition of buffering salts, such as NaOH, to correct the pH-value and prevent VO_2 dissolution in a real hybrid super-capacitor application.

Declaration of competing interest

The authors declare that they have no known competing financial interests or personal relationships that could have appeared to influence the work reported in this paper.

CRediT authorship contribution statement

Simon Lindberg: Investigation, Formal analysis, Conceptualization, Writing - original draft. **Ndeye Maty Ndiaye:** Formal analysis, Conceptualization. **Ncholu Manyala:** Writing - review & editing, Funding acquisition, Supervision. **Patrik Johansson:** Writing - review & editing, Funding acquisition, Supervision. **Aleksandar Matic:** Writing - review & editing, Supervision, Conceptualization, Project administration.

Acknowledgements

This research was supported by the Swedish Energy Agency “Batterifonden” grant #39042−1.

References

[1] D.P. Dubal, O. Ayyad, V. Ruiz, P. Gomez-Romero, Hybrid energy storage: the merging of battery and supercapacitor chemistries, Chem. Soc. Rev. 44 (2015) 1777−1790, https://doi.org/10.1039/C4CS00266K.
[2] V. Augustyn, P. Simon, B. Dunn, Pseudocapacitive oxide materials for high-rate electrochemical energy storage, Energy Environ. Sci. 7 (2014) 1597, https://doi.org/10.1039/c3ee44164d.
[3] P. Simon, A. Burke, Nanostructured carbons: double-layer capacitance and more, Electrochem. Soc. Interface. 17 (2008) 38−43, https://doi.org/10.1016/j.carbon.2005.06.046.
[4] K.O. Oyedotun, T.M. Masikhwa, S. Lindberg, A. Matic, P. Johansson, N. Manyala, Comparison of ionic liquid electrolyte to aqueous electrolytes on carbon nanofibres supercapacitor electrode derived from oxygen-functionalized graphene, Chem. Eng. J. 375 (2019), https://doi.org/10.1016/j.cej.2019.121906.
[5] X. Gu, J. Yue, L. Li, H. Xue, J. Yang, X. Zhao, General synthesis of MnO_x (MnO_2, Mn_2O_3, Mn_3O_4, MnO) hierarchical microspheres as lithium-ion battery anodes, Electrochim. Acta 184 (2015) 250−256, https://doi.org/10.1016/j.electacta.2015.10.037.
[6] C. Zhong, Y. Deng, W. Hu, J. Qiao, L. Zhang, J. Zhang, A review of electrolyte materials and compositions for electrochemical supercapacitors, Chem. Soc. Rev. 44 (2015) 7484−7539, https://doi.org/10.1039/C5CS00303B.
[7] X. Yu, D. Ruan, C. Wu, J. Wang, Z. Shi, Spiro-(1,1′)-bipyrrolidinium tetrafluoroborate salt as high voltage electrolyte for electric double layer capacitors, J. Power Sources 265 (2014) 309−316, https://doi.org/10.1016/j.jpowsour.2014.04.144.
[8] M.P. Bichat, E. Raymundo-Piñero, F. Béguin, High voltage supercapacitor built with seaweed carbons in neutral aqueous electrolyte, Carbon N. Y. 48 (2010) 4351−4361, https://doi.org/10.1016/j.carbon.2010.07.049.
[9] F. Zhang, T. Zhang, X. Yang, L. Zhang, K. Leng, Y. Huang, Y. Chen, A high-performance supercapacitor-battery hybrid energy storage device based on graphene-enhanced electrode materials with ultrahigh energy density, Energy Environ. Sci. 6 (2013) 1623, https://doi.org/10.1039/c3ee40509e.
[10] L. Suo, F. Han, X. Fan, H. Liu, K. Xu, C. Wang, “Water-in-Salt” electrolytes enable green and safe Li-ion batteries for large scale electric energy storage applications, J. Mater. Chem. A. 4 (2016) 6639−6644, https://doi.org/10.1039/C6TA00451B.
[11] D. Reber, R.-S. Kühnel, C. Battaglia, High-voltage aqueous supercapacitors based on NaTFSI, Sustain. Energy Fuels (2017), https://doi.org/10.1039/C7SE00423K.
[12] L. Suo, O. Borodin, Y. Wang, X. Rong, W. Sun, X. Fan, S. Xu, M.A. Schroeder, A.V. Cresce, F. Wang, C. Yang, Y.S. Hu, K. Xu, C. Wang, “Water-in-Salt” electrolyte makes aqueous sodium-ion battery safe, green, and long-lasting, Adv. Energy Mater. 7 (2017) 1−10, https://doi.org/10.1002/aenm.201701189.
[13] O. Borodin, L. Suo, M. Gobet, X. Ren, F. Wang, A. Faraone, J. Peng, M. Olguin, M. Schroeder, M.S. Ding, E. Gobrogge, A. Von Wald Cresce, S. Munoz, J.A. Dura, S. Greenbaum, C. Wang, K. Xu, Liquid structure with nano-heterogeneity promotes cationic transport in concentrated electrolytes, ACS Nano 11 (2017) 10462−10471, https://doi.org/10.1021/acsnano.7b05664.
[14] L. Suo, O. Borodin, T. Gao, M. Olguin, J. Ho, X. Fan, C. Luo, C. Wang, K. Xu, “Water-in-salt” electrolyte enables high-voltage aqueous lithium-ion chemistries, Science 80 (2015) 350, https://doi.org/10.1126/science.aab1595.
[15] Y. Zhang, J. Zheng, T. Hu, F. Tian, C. Meng, Synthesis and supercapacitor electrode of VO2(B)/C core-shell composites with a pseudocapacitance in aqueous solution, Appl. Surf. Sci. 371 (2016) 189−195, https://doi.org/10.1016/j.apsusc.2016.02.199.
[16] J. Shao, X. Li, Q. Qu, H. Zheng, One-step hydrothermal synthesis of hexangular starfruit-like vanadium oxide for high power aqueous supercapacitors, J. Power Sources 219 (2012) 253−257, https://doi.org/10.1016/j.jpowsour.2012.07.045.
[17] N.M. Ndiaye, T.M. Masikhwa, B.D. Ngom, M.J. Madito, K.O. Oyedotun, J.K. Dangbegnon, N. Manyala, Effect of growth time on solvothermal synthesis of vanadium dioxide for electrochemical supercapacitor application, Mater. Chem. Phys. 214 (2018) 192−200, https://doi.org/10.1016/j.matchemphys.2018.04.087.
[18] M. Zhang, J.R. Dahn, Electrochemical lithium intercalation in $V0_2$(B) in aqueous electrolytes, J. Electrochem. Soc. 143 (1996) 2730−2735, https://doi.org/10.1002/adma.200600065.
[19] L. Deng, G. Zhang, L. Kang, Z. Lei, C. Liu, Z.H. Liu, Graphene/VO_2 hybrid material for high performance electrochemical capacitor, Electrochim. Acta 112 (2013) 448−457, https://doi.org/10.1016/j.electacta.2013.08.158.
[20] A. Balducci, D. Belanger, T. Brousse, J.W. Long, W. Sugimoto, Perspective—a guideline for reporting performance metrics with electrochemical capacitors: from electrode materials to full devices, J. Electrochem. Soc. 164 (2017) A1487−A1488, https://doi.org/10.1149/2.0851707jes.
[21] S.T. Vindt, E.M. Skou, The buffer effect in neutral electrolyte supercapacitors, Appl. Phys. Mater. Sci. Process 122 (2016) 1−6, https://doi.org/10.1007/s00339-015-9563-8.
[22] R.B. Rakhi, D.H. Nagaraju, P. Beaujuge, H.N. Alshareef, Supercapacitors based on two dimensional VO_2 nanosheet electrodes in organic gel electrolyte, Electrochim. Acta 220 (2016) 601−608, https://doi.org/10.1016/j.electacta.2016.10.109.
[23] R.J. Gilliam, J.W. Graydon, D.W. Kirk, S.J. Thorpe, A review of specific conductivities of potassium hydroxide solutions for various concentrations and temperatures, Int. J. Hydrogen Energy 32 (2007) 359−364, https://doi.org/10.1016/j.ijhydene.2006.10.062.
[24] J. Mähler, I. Persson, A study of the hydration of the alkali metal ions in aqueous solution, Inorg. Chem. 51 (2012) 425−438, https://doi.org/10.1021/ic2018693.